Optical and Physical Requirements for Fluid Particles Marking Trailing Vortices from Aircraft

Lloyd H. Back*
Jet Propulsion Laboratory, Pasadena, Calif.

A theoretical study of the optical and physical requirements of marking trailing vortices that emanate from aircraft wings was carried out by considering particulate light-scattering properties, ability of particles to follow trailing vortices, and survival time of particles to vortex dissipation. Liquid droplets undergoing evaporation and molecular dispersion were investigated. Droplets should have lifetimes of about 300 sec. Droplet size should be about 1 μ to maximize light scattering with the minimum mass of liquid required. Droplets of this small size would spiral outward very slowly and essentially remain in the vortex cores. Nontoxic hygroscopic liquids, having an affinity for moisture in the air, have been identified. These liquids have relatively low vapor pressures of order 10^{-5} mm Hg that would insure droplet persistence long enough to mark trailing vortices.

Nomenclature

A = cross-sectional area of a trailing vortex
b = wingspan
c_{p_l} = vapor specific heat
d_p = particle diameter
D = binary diffusion coefficient
F = function defined in Eq. (24a)
G = scattering function
h_{fg} = latent heat of vaporization
I_s = intensity of scattered light
I_0 = intensity of incident light
k = thermal conductivity
L = lift force
m = index of refraction
m_v = mass of particles injected into a trailing vortex
$\dot{m}_v$ = mass flow rate
m_p = mass of a particle
$\dot{m}_p$ = evaporation rate
M_l = molecular weight
n = number density of particles
p_{l_0} = vapor pressure of liquid
p_{l_∞} = partial pressure of vapor if present in surrounding air
q = relative particle size parameter, Eq. (3)
r = radial distance
r_c = vortex core radius
r_p = particle radius
R = distance from particle to observer
R_l = gas constant of vapor
R_u = universal gas constant
t = time
t_E = evaporation time
t_p = vortex persistence time
T = temperature
T_0 = wet bulb temperature of liquid
T_∞ = ambient air temperature
u_p = axial velocity of particle
u_∞ = flight speed
v_r = particle radial velocity
v_Θ = particle tangential velocity
V_p = particle volume
V_s = scattering volume
w_l = mass fraction of vapor
w_Θ = tangential velocity of vortex flow
W = plane weight
x = axial distance
η = scaling parameter
Θ = view or scattering angle
λ = wavelength
μ_f = viscosity of air
ρ = mass density of particles
ρ_f = density of air
ρ_p = density of a particle
Γ_0 = circulation

Subscript

i = initial condition

Superscript

$\bar{(\ )}$ = average value

Received Jan. 22, 1975; revision received July 31, 1975. The author is indebted to E. Bate, Jr., of AeroVironment, Inc., Pasadena, Calif. who carried out the numerical calculations of particle trajectories under Contract 953964 and to R. Rhein, a chemist, who identified several liquids of interest in the study. This work presents the results of one phase of research carried out in the Propulsion Division of the Jet Propulsion Laboratory, California Institute of Technology, under Contract NAS 7 – 100, sponsored by NASA.

Index categories: Jets, Wakes, and Viscid – Inviscid Flow Interactions; Multiphase Flows; Aricraft Aerodyanmics (including Component Aerodynamics).

*Member Technical Staff. Associate Fellow AIAA.

I. Introduction

THE flowfield in the wake of large aircraft is a significant hazard to smaller planes that fly into this region[1,2] and experience rolling moments and pitch disturbances in crossing vortices. This hazard is caused by the comparatively strong trailing vortices leaving the trailing edge of a wing[3] particularly near wing-tips and deflected flaps. These contra-rotating vortices whose strength is proportional to the weight of the plane can persist for a significant time behind large aircraft before they dissipate into a harmless turbulent state.[4,5] This hazard is particularly great during landing at airports that must accommodate a large number of flights thus necessitating flight within these wakes where low power and proximity to the ground reduce a smaller plane's chance for recovery from aerodynamic forces imparted by the trailing vortices.

The objective of this investigation is to theoretically establish the optical and physical requirements of a nonpolluting material to mark trailing vortices, for operational use and study purposes. The main emphasis is on visible detection of scattered sunlight from particulates injected at the trailing edge of wings. Important particulate characteristics are scattering properties (particle size, refractive index, view angle), ability to follow trailing vortices (particle size, refractive index, view angle), ability to follow trailing vortices (particle size, density, vortex characteristics), survival time to vortex dissipation (vaporization characteristics), ultimate dispersibility, and minimization of the mass of particulates required. The study pertains to liquid droplets undergoing evaporation and molecular dispersion.

General features of trailing vortices reveal separation distances approximately equal to the wingspan b after roll up of the trailing vortex sheet, core radii r_c (location of peak tangential velocity), a few percent of the wingspan b, and peak tangential velocities less than flight speed u_∞.[6-9] Basic modes of vortex decay known to exist are by viscous dissipation, vortex instability, vortex breakdown, and atmospheric interactions[10-14] although little is known about the decay of trailing vortices behind large aircraft under general atmospheric conditions. Breakdown of trailing vortices into a train of vortex rings described by Crow[11] is often observed under calm conditions. With flaps deployed the structure of trailing vortices is even more complex. Patterson[15] has observed the interaction of the flap vortex pair and wing-tip vortex resulting in a spiraling vortex system with a common center of rotation in model B−747 tests. It would appear that establishing the requirements of a marker material cannot depend on detailed knowledge of the flow structure of trailing vortices since such informaiton is not at hand. However, it is possible to define the optical and physical requirements of a marker material by approximate analyses as presented herein.

II. Optical Requirements

The optical requirements for a marker material were established by using Mie scattering theory[16,17] and the conservation principle for the mass flow rate of particles injected into a trailing vortex. These aspects are described separately in this section for completeness and then combined to obtain a scattering parameter that indicates the optimum size for particles.

Mie Scattering Theory

Mie originally solved Maxwell's field equations for the scattering of a plane electromagnetic wave of intensity I_0 and wavelength λ from a isotropic sphere of diameter d_p (Fig.1). The intensity I_s of the scattered electromagnetic wave at an angle θ measured from the forward direction of propagation of the incident beam and at a distance R from the particle in the far field where the inverse square law applies is given by (e.g. Ref. 18, p. 129)

$$\frac{I_s}{I_0} = \bar{n} V_s \left[\frac{1}{4\pi^2} \left(\frac{\lambda}{R} \right)^2 G \right] \tag{1}$$

The term in brackets represents the scattered intensity from one particle, and when multiplied by the number density $\bar{n}$ of particles and the scattering volume V_s, i.e., for N particles, gives the scattered intensity from the volume V_s. Since relatively dilute particle concentrations are of interest the condition for independent scattering given by Van de Hulst,[18] i.e., for particle separation distances greater than about three particle radii, should be valid so that Eq. (1) is applicable. Treating the particles as spherical is also believed to be a reasonable assumption for small liquid droplets on the order of 1 μ in size which will be seen to be of interest subsequently.

For an incident unpolarized electromagnetic wave such as sunlight the function G in Eq. (1) is given by

$$G = \frac{1}{2} \left(i_\perp + i_\parallel \right) \tag{2}$$

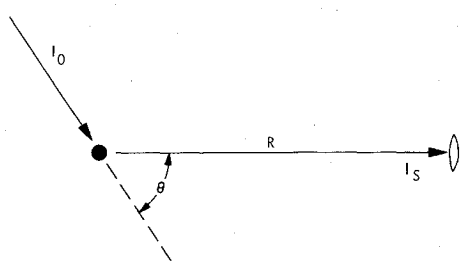

Fig.1 Scattering configuration.

where the normalized scattered intensities $i_\perp$ and $i_\parallel$ are perpendicular and parallel to the plane of observation, respectively; they often appear in the literature as i_1 and i_2. The scattered electromagnetic wave is partially polarized. The scattered intensities are obtained from infinite series solutions of the wave equation involving Legendre, Bessel and Hankel functions corresponding to partial waves. From these solutions the function G is found to depend upon the relative size of the particle compared to the wavelength λ of the incident beam, i.e.,

$$q = \frac{\pi d_p}{\lambda} \tag{3}$$

the view or scattering angle Θ, and the index of refraction m, in functional notation

$$G(q, \Theta, m)$$

For dielectric or nonabsorbing particles that are of interest, m is real, not complex.

Mie theory is quite general, covering the range of sizes of very small particles (relative to the incident beam wavelength λ) in the Rayleigh regime to large particles relative to λ for which classical geometric optics apply. Mie's theory has been confirmed experimentally, e.g., see Paranjpe, et al.,[19] La Mer and coworkers,[20] and Heller.[21]

Mass Flow Rate

The mass flow rate of particles injected steadily into a trailing vortex is given by

$$\dot{m}_v = \bar{\rho} \bar{u}_p A \tag{4}$$

where the barred quantities are average values for the mass density of particles and axial velocity across the cross-sectional area A through which particles flow axially. The mass m_v of particles injected over a period of time Δt to mark the trailing vortex is simply

$$m_v = \dot{m}_v \Delta t \tag{5}$$

The number density $\bar{n}$ of particles can then be written as follows from its definition and by using Eqs. (4) and (5)

$$\bar{n} = \frac{\bar{\rho}}{m_p} = \frac{\bar{\rho}}{\rho_p V_p} = \frac{m_v}{\Delta t \bar{u}_p A \rho_p V_p} \tag{6}$$

where m_p, ρ_p and V_p are the mass, density and volume of a particle, respectively.

Particle Size

The intensity of scattered light is given as follows upon substitution of Eq. (6) into Eq. (1)

$$\frac{I_s}{I_o} = \frac{1}{4\pi^2} \frac{m_v}{\Delta t \bar{u}_p} \left(\frac{\lambda}{R} \right)^2 \frac{V_s}{A} \frac{1}{\rho_p} \left(\frac{G}{V_p} \right) \tag{1a}$$

To minimize the mass m_v of particles required, the scattering function G divided by the particle volume V_p should be as large as possible. The other quantities are more or less fixed for a given set of observation and flight conditions. To first order, V_s/A is the length ℓ_s of trailing vortex discernible to the eye; the density ρ_p of liquid droplets of interest differs little from unity in g/cm^3, and axial particle velocities are near flight speeds. The eye sensitivity curve is essentially gaussian in the visible region from 0.4 to 0.7 μ and has a peak value at a wavelength of 0.555 μ although the peak varies somewhat from person to person.[22]

Since the particle volume is proportional to the cube of the relative size parameter q, then the scattering parameter of im-

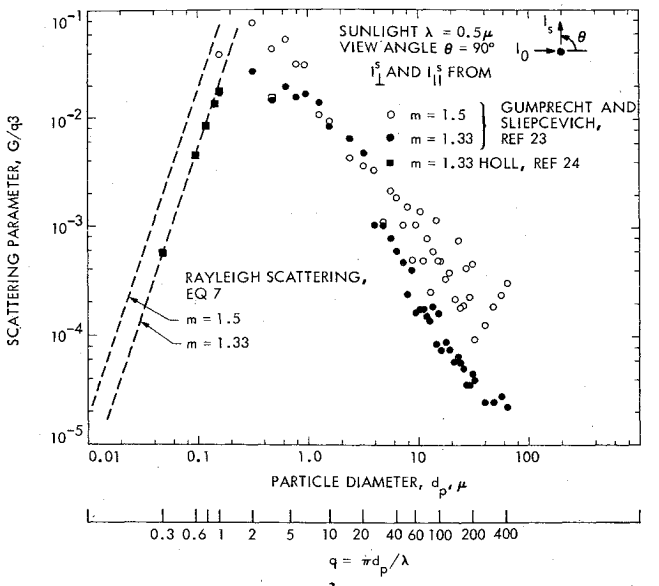

Fig.2 Scattering parameter G/q^3 from Mie theory, view angle 90°.

portance is G/q^3 in nondimensional form. Calculated values of the scattering parameter obtained from values of $I^s_\perp$ and $I^s_\parallel$ given in Refs. 23 and 24 are shown in Fig. 2 as a function of particle size at a 90° view angle for sunlight at a wavelength of 0.5 μ. For relatively small particles the calculations check with the analytical result (first term in the series solution) for Rayleigh scattering as they should

$$\frac{G}{q^3} = \frac{I}{2} q^3 \left(\frac{m^2-1}{m^2+2}\right)^2 (1+\cos^2\theta) \tag{7}$$

In the Rayleigh regime, values of the scattering parameter increase with particle size. Peak values of the scattering parameter correspond to particles about 0.5 μ diam. Larger particles lead to a decrease in the magnitude of the scattering parameter, e.g., the reduction is by a factor about 100 for 30 μ diam particles. Of note is that the scatter of the calculated values is associated with the partial wave contributions and not with the accuracy of the solutions even at large values of q where increasingly more terms in the series solution require evaluation.

The scattering parameter increases with the value of the refractive index m as indicated in Fig. 2. A value of $m=1.33$ corresponds to water droplets in particular, and a value of $m=1.5$ is typical of smoke oil particles.[25]

At smaller view angles Θ, i.e., in the forward direction, the magnitude of the scattering parameter increases appreciably and there is a shift in the peak to particles nearer 1 μ diam as shown in Fig. 3. There is little difference in the average value for backscattering from 90° to 180° compared to that at 90°. In general, the view angle between observer and incident beam depends upon the relative orientation of the sun, trailing vortex and observer. Sky lighting is also important in providing contrast for light scattered from particles. Although a variety of observational situations will occur in practice, it would appear, nevertheless, that particles on the order of 1 μ in size are desirable for maximum light scattering.

III. Particle Trajectories

Numerical calculations of particle trajectories were carried out[26] based on a number of simplifying assumptions to determine if particles would remain in the vortex core for marking times of interest. For particles as small as 1 μ, the time to accelerate a particle to vortex flow speeds was considered to be extremely small. By neglecting radial accelerations, the radial force balance on a particle using the Stokes' flow assumption and including the radial buoyancy force reduced to the

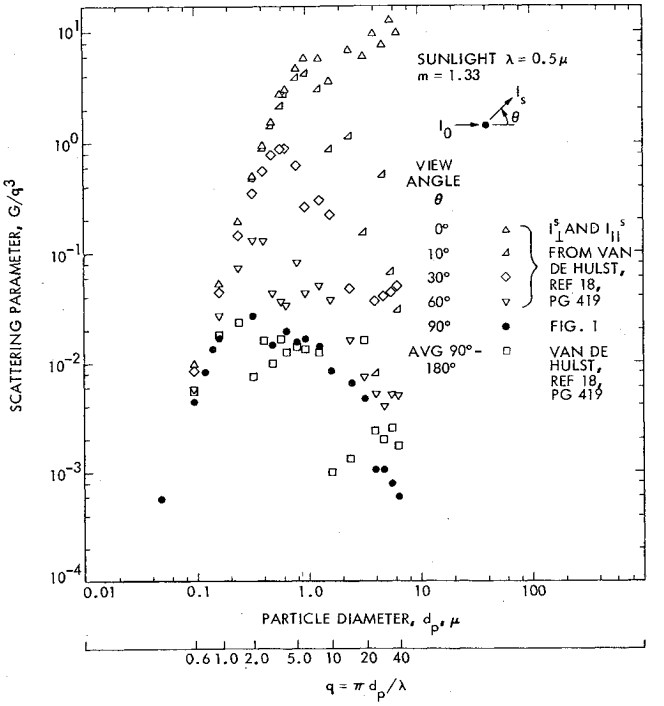

Fig.3 Scattering parameter G/q^3 variation with view angle.

following form in a rotating flow with tangential velocity w_Θ and negligible radial velocity w_r

$$-m_p \frac{(\rho_p-\rho_f)}{\rho_p} \frac{v_\theta^2}{r} = 6\pi\mu_f r_p(-v_r) \tag{8}$$

In this relation the particle velocities in the radial r-direction and tangential direction are v_r and v_Θ, respectively, and ρ_f and μ_f are the density and viscosity of air, respectively. For a spherical particle of mass $m_p=\rho_p(4\pi/3)\, r_p^3$ moving at a tangential velocity v_Θ equal to the tangential flow velocity w_Θ, the radial velocity v_r is

$$v_r = \frac{4}{18} \frac{(\rho_p-\rho_f)}{\mu_f} \frac{r_p^2}{r} w_\theta{}^2 \tag{9}$$

Specification of the tangential flow velocity w_Θ then allows the calculation of radial particle displacement from $v_r=dr/dt$ and axial location from $x=u_\infty t$ as a first approximation for particles initially at various radii r_i, ignoring particle evaporation. In the calculations, a viscous vortex flow was assumed with a simple, analytical expression for the tangential flow velocity given by

$$w_\theta = \frac{\Gamma_0}{2\pi r}\left[1-\exp\{(-5/4)(r/r_c)^2\}\right] \tag{10}$$

where Γ_0 is the circulation, although some measured velocities, e.g., Refs. 8 and 27, could have been used as well.

The number density of particles determined by considering the radial advection of an expanding annular shell of particles which always contains the same number of particles since diffusion is neglected is given by

$$n = n_i \frac{r_i}{r} \frac{v_{r_i}}{v_r} \tag{11}$$

In this relation r is the time-dependent radius obtained by integration of Eq. (9) and the subscript i denotes the initial particle conditions.

This formulation was cast in nondimensional form where in radial location is normalized by core radius r/r_c and axial

distance by wingspan x/b, and the circulation was calculated from the Jukowski lift relation for elliptic wing loading

$$L = W = \frac{\pi}{4}\rho_f u_\infty b\Gamma_0 \tag{12}$$

The particle number density at a downstream location x/b depends upon particle characteristics, size and density; vortex characteristics as governed by plane weight W, wingspan b, flight speed u_∞, and ratio of core radius to wingspan r_c/b; ambient conditions; and initial distribution of particles. Aircraft scaling characteristics depend upon the following group of quantities to which the particle radial velocity is related

$$\eta = \frac{W^2}{u_\infty{}^3 b^5 (r_c/b)^4} \tag{13}$$

i.e., in nondimensional form

$$\frac{d(r/r_c)}{d(x/b)} = \frac{8}{9\pi^4}\eta\frac{(\rho_p-\rho_f)}{\mu_f\rho_f^2}r_p^2\frac{1}{(r/r_c)^3}$$

$$\times[1-\exp\{-(5/4)(r/r_c)^2\}]^2 \tag{14}$$

Calculations are shown in Fig. 4 for a B−747 at a downstream distance of $x/b = 135$ [8km (5 mi) or at a time of 92 sec]. The figure shows predictions for 1, 2, and 5 μ diam particles initially at evenly spaced particle cloud radii r_i/r_c. For larger particles, the particle cloud becomes less dense near the center of the vortex and forms a relatively denser ring of particles at the outer edge of the cloud. For smaller particles of 1 μ diam, the calculations indicate near uniformity in the number density of particles across the flow. In this case, particles would spiral outward very slowly and essentially remain in the vortex core. These calculations actually overestimate the centrifugal action on the particles since vortex decay and particle evaporation were not taken into account. The estimated first-order effect of turbulent diffusion would be to reduce the calculated loss of partricles in the core region since diffusion then would be from a region of higher to lower particle number densities (Fig.4) and thus be radially inward, thereby balancing the radially outward convection of particles in the core region.

The visual appearance of the particle-marked vortices is directly related to the particle number density distribution in the vortices via the Abel integral equation

$$n(\xi) = 2\int_\xi^{r_e}\frac{n(r)r}{(r^2-\xi^2)^{1/2}}dr \tag{15}$$

where ξ is the distance from the vortex center to the visual path and r_e is the outer edge of the particle cloud.

Although these calculations are approximate, they do indicate that particles about 1 μ in size, desirable for maximum light scattering, should remain in the vortex cores for marking times discussed subsequently.

IV. Particle Evaporation Times

The time for spherical droplets to evaporate obtained from the evaporation rate

$$\dot{m}_p = -\frac{dm_p}{dt} = -\rho_p\frac{dV_p}{dt} = -\rho_p 4\pi r_p{}^2\frac{dr_p}{dt} \tag{16}$$

is given by

$$t_E = 4\pi\rho_p\int_o^{r_{pi}}\frac{r_p^2\,dr_p}{\dot{m}_p} \tag{17}$$

Estimates of evaporation time were made for quasi-steady diffusion controlled evaporation for which the solution of the

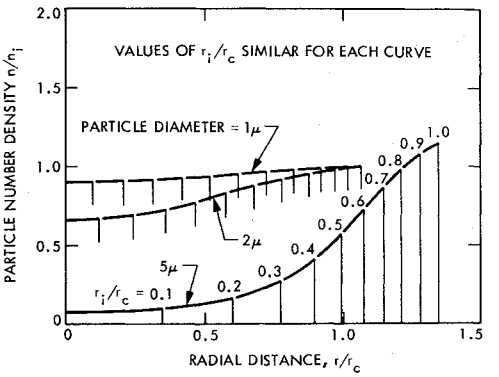

Fig. 4 Particle density distribution for B-747 at downstream distance $x/b = 135$ (Ref. 26), $W = 322{,}000$ kg (710,000 lb), $b = 59.7$ m (196 ft), $U_\infty = 87.6$ m/sec (196 mph), $r_c = 0.444$, $\rho_p = 1$ g/cm^3, uniform initial distribution.

diffusion equation for a binary mixture of the vapor and air is given as follows[28]

$$\dot{m}_p = 4\pi\bar{\rho}\bar{D}r_p\ln\left(\frac{1-w_{1_\infty}}{1-w_{1_o}}\right) \tag{18}$$

In this relation w_1 is the mass fraction of the vapor in the film surrounding the droplet, w_{1_0} being the value at the liquid-vapor interface and $w_{1\infty}$ in the surrounding air if the same vapor is present there too. The barred quantities refer to average values for the film density and binary diffusion coefficient D.

For relatively small mass fractions of vapor, a situation of interest herein, Eq. 18 reduces to the Langmuir relation

$$\dot{m}_p \cong \frac{4\pi\bar{D}r_p}{R_1\bar{T}}(p_{1_o}-p_{1_\infty}) \tag{18a}$$

where p_{1_0} is the vapor pressure of the liquid droplet at the wet bulb temperature T_0; p_{1_∞} is the partial pressure of the vapor if present in the surrounding air; $\bar{T}$ is the average temperature surrounding the droplet; and R_1 is the gas constant of the vapor R_u/M_1. Langmuir's relation has been verified experimentally provided that the droplets are not so small that evaporation kinetics become important in controlling evaporation (Ref. 25, p. 89). This expression is used here in even for droplets of 1 μ diam for which estimated evaporation times discussed subsequently may be too low by 100%. Compensation for the uncertainty in actual evaporation times is made later. Forced convection effects which would reduce evaporation times are believed to be insignificant because of the small size of the particles and negligibly small slip velocities, i.e., Reynolds numbers would be much less than unity, and thus transport of vapor to the surrounds essentially would be by diffusion and radial convection.

For droplet evaporation at a constant wet bulb temperature, insertion of Langmuir's relation Eq. 18a into Eq. 17 and carrying out the integration gives the evaporation time as

$$t_E = \frac{1}{8}\frac{R_1\bar{T}}{\bar{D}}\frac{\rho_p}{(p_{1_o}-p_{1_\infty})}d_{p_i}^2 \tag{19}$$

where d_{p_i} is the initial diam of the droplet.

In order to estimate evaporation times, the wet bulb temperature of the droplet needs to be determined so that the vapor pressure is then specified, i.e., $p_{1_0}(T_0)$. For droplets of interest, the effect of curvature on the vapor pressure of a drop is believed to be negligible[29]. The wet bulb temperature was determined by using the solution of the thermal energy equation (Ref. 28)

$$\dot{m}_p = \frac{4\pi\bar{k}}{\bar{c}_{p_1}}r_p\ln\left[1+\frac{\bar{c}_{p_1}}{h_{fg}}(T_\infty - T_o)\right] \tag{20}$$

in conjunction with the diffusion solution Eq. 18 which gives the following implicit relation for relatively small mass fractions of vapor and negligible changes in sensible enthalpy across the vapor film compared to the latent heat

$$\frac{\bar{D}}{R_l \bar{T}}(p_o - p_{l_\infty}) \cong \frac{\bar{k}}{h_{fg}}(T_\infty - T_o) \tag{21}$$

In these equations T_∞ is the ambient air temperature, h_{fg} is the latent heat of vaporization of the liquid droplet, c_{pl} is the vapor specific heat and k is the film thermal conductivity. The wet bulb temperature – vapor pressure relationship given in Eq. 21 is independent of droplet size.

Calculations were carried out for 1 μ diam water droplet in dry air at $T_\infty = 70°F$ (21°C) and $p_0 = 1$ atm. The wet bulb temperature of the droplet determined from Eq. 21 was $T_0 = 40°F$(4.4°C) and the vapor pressure $p_{l_0} = 6.3$ mm Hg. The estimated evaporation time obtained from Eq. 19 was only about 1 msec. Even in air at 50% relative humidity for which the wet bulb temperature would be 58°F. (14.4°C), the evaporation time is only about twice as large.

These calculations indicate that the lifetime of small water droplets 1 μ in size injected into trailing vortices would be too short to effectively mark vortices because of the relatively high vapor pressure of water and the corresponding rapid droplet evaporation rate. Even water droplets 30 μ in size would have lifetimes less than 1 sec since $t_E \propto d_{p_i}{}^2$. Clearly, liquid droplets with relatively low vapor pressures are required as discussed in Section VI.

V. Vortex Persistence Times

The decay in the strength of trailing vortices from large aircraft and the hazard to smaller aircraft is not known well enough to calculate a time at which trailing vortices cease to be dangerous with too much certainty.

Some idea of the time for vortices to persist until linking occurs as a breakdown mode was calculated from the natural time scale for the growth of waves[11] i.e., the time for the undisturbed vortices to descend a distance equal to their separation, and a dimensionless time t^* defined by Moore, Ref. 30.

$$t_p = 2\pi \frac{b^2}{\Gamma_0} t^* \tag{22}$$

By using a value of $t^* \simeq 2.5$ determined by Moore from nonlinear, vortex linking theory and values of the circulation from the Jukowski lift relation (Eq. 12,) the time t_p becomes

$$t_p = \frac{\pi^2}{2} t^* \frac{\rho_f u_\infty b^3}{W} \tag{23}$$

Calculated values of t_p are shown in Fig. 5 for various aircraft. Information on aircraft wing span, weight, and flight speed was obtained from Refs. 31 and 32. Estimated times for larger aircraft range from 60 to 120 sec. For the B – 747 in particular, there is reasonably good agreement with an observed value of 100 sec reported by Condit and Tracy.[33] The effect of atmospheric turbulence is to shorten persistence times.[14] Conversely, under very calm conditions, vortices from a large aircraft like the B – 747 may persist up to 16 km (10 mi) downstream or for about 180 sec. With flaps deployed, vortices often decay by viscous dissipation and breakdown rather than by linking.

These observations indicate that persistence times can vary greatly. For a marking material to be effective, it must persist long enough to exceed vortex decay times measured.

VI. Search for Liquids

A conservative estimate of the time for a particle to evaporate was taken to be 300 sec based on the preceding considerations. This lifetime would exceed estimatd vortex persistence times and allow for a factor of safety in the uncertainty in actual evaporation times associated with evaporation kinetics of very small liquid droplets.

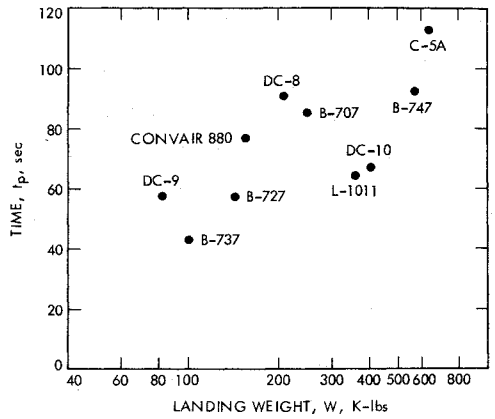

Fig. 5 Estimated vortex persistence times for various aircraft-linking mode.

An estimate was then made of the vapor pressure 1 μ diam liquid droplets should have to persist for this required time by using Eq. (19)

$$p_{l_0} = \frac{1}{8} \frac{R_u \bar{T}}{M_l \bar{D}} \rho_p \frac{d_{p_i}^2}{t_E} \tag{24}$$

This was carried out in an approximate way since the molecular weight, diffusion coefficient, and droplet density of the unspecified liquid and its vapor are not known a priori. By referencing these quantities to a water droplet for convenience, the vapor pressure was expressed as

$$p_{l_0} = \frac{1}{8} \frac{R_u}{M_w} \frac{\bar{T}}{\bar{D}_w} \rho_{p_w} \frac{d_{p_i}^2}{t_E} F \tag{24a}$$

where

$$F = \frac{M_w}{M_l} \frac{\bar{D}_w}{\bar{D}} \frac{\rho_p}{\rho_{p_w}}$$

The calculated value of p_{l_0}/F at a temperature of 70°K (21°C) is 1.5×10^{-5} mm Hg. Since values of F turn out to range from 0.5 to 0.8 for the liquids of interest, the desired vapor pressure is on the order of 10^{-5} mm Hg. To broaden the base of the study, a range of vapor pressures from 10^{-3} to 10^{-6} mm Hg and a range of temperatures from 0 to 35°C were investigated.

The study involved using the Clausius-Clapeyron relation to extend the available information on vapor pressure-temperature data for liquids to the relatively low vapor pressures of interest. Vapor pressure-temperature data are usually given at pressures of 1 mm Hg and above.[34] The $\ln p_{l_0}$ vs $1/T$ was plotted and then a curve was fit to the higher pressure data allowing for the variation of latent heat with temperature when extended to lower vapor pressures. The curve fit was of the form

$$T \ln p_{l_0} = A + BT + CT^2 + DT^3 \tag{25}$$

where the leading coefficient $A = h_{fg0}/R_l$ and the coefficients B and C involve the variation of latent heat with temperature. The last term DT^3 was found to be negligible.

The results of the study are shown in Fig. 6 in terms of vapor pressure vs temperature for several liquids. Table 1 gives relevant information on the physical properties of these liquids and their vapors (Ref. 34 and 35).

Tetraethylene glycol may be a suitable candidate. It is nontoxic, commercially available, and has an estimated vapor pressure of 1.2×10^{-5} mm Hg at 20°C, a refractive index of 1.45 and a density of 1.12 g/cm^3. It is also hygroscopic, having an affinity for moisture in the air.

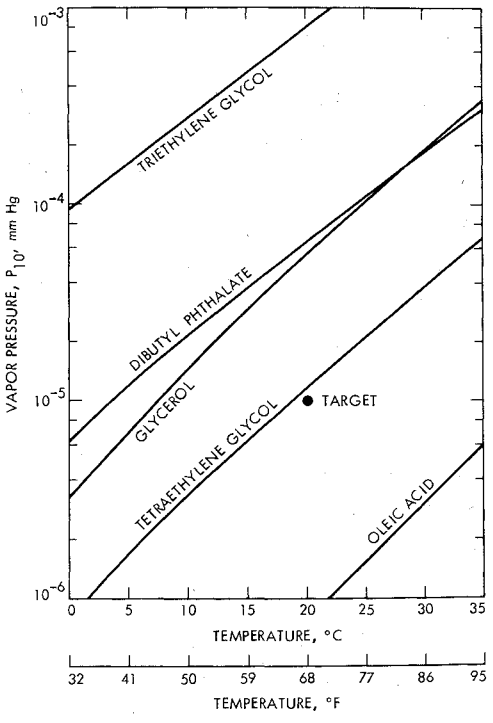

Fig. 6 Vapor pressure vs temperature for several liquids.

At various ambient air temperatures, mixtures of hygroscopic liquids could be employed to attain the desirable vapor pressure and thus evaporative characteristics. Wet bulb temperatures would be imperceptibly below the ambient air temperature for these relatively low vapor pressure liquids as deduced from Eq. (21). Ultimate dispersibility and fate of marker molecules in the atmosphere require subsequent study.

VII. Liquid Droplet Flow Rates and Smoke Oil Observations

Even though liquid droplet flow rates cannot be established a priori because of uncertainties in visual response and contrast associated with sky lighting, available information on other marker materials does provide some guidance in estimating required flow rates.

Flight tests recently conducted at NASA Flight Research Center, Edwards, Calif. with six corvus smoke oil generators mounted at the wing tips and at the outer edges of the inboard and outboard flap locations of a B – 747, indicated that flow rates of about 15 g/sec (2 lb/min) from each generator marked the trailing vortices very well in a cruise configuration.[36,37] Since the liquids of interest herein have refractive indices near that of oil droplets which are also believed to be of order 1 μ in size, then comparable flow rates should also provide adequate marking for the liquids considered.

Flight tests, however, have indicated that wing flap extension on the B-727 aircraft had a pronounced effect on the characteristics and persistence of the trailing vortex system. In the landing configuration with 30° flap deflection, the interaction of the flap vortices with the wing-tip vortices created a vortex system that was much larger in diam than the vortex system associated with the clean configuration (no flap extension). This interaction appeared to occur within a few span lengths behind the wing wherein the smoke entrained in the tip vortex appeared to wrap around the flap vortex, thereby diffusing the smoke. The vortex became invisible to the photographer at about 40 sec before any onset of breakdown, apparently as a result of the smoke becoming so diffuse that it no longer marked the vortex. Whereas the clean wing resulted in a concentrated, well-defined vortex core, the vortex tended to become more diffuse and created less of an upset on an encountering aircraft when the flaps were lowered. It is not clear whether the marking materials considered herein would improve the vortex system visibility in this situation when the vortex system is larger in diam since the particles would also be spread out more in following the vortex flow. Higher droplet flow rates may be required to increase the number density of light scattering particles in such vortex systems.

Of note is that evaporation times for corvus oil droplets would be much larger than those considered herein because of the relatively low vapor pressure, judged to be less than 10^{-6} mm Hg. Oil smokes used in air shows end up showering the ground and spectators with oil droplets. Oils, including dibutyl phthalate, also are not hygroscopic.

VIII. Conclusions

The optical and physical requirements of a market material have been defined for detection of trailing vortices. Particles on the order of 1 μ in size are desirable for maximum light scattering with the minimum mass of particulates. Particles of

Table 1 Physical properties of several liquids and their vapors

	Tetra – ethylene Glycol	Glycerol	Triethylene-Glycol	Dibutyl phthalate	Oleic-Acid
Chemical formula	$C_8H_{18}O_5$	$C_3H_8O_3$	$C_6H_{14}O_4$	$C_{16}H_{22}O_4$	$C_{18}H_{34}O_2$
Molecular weight	194	92	150	278	314
Normal boiling point at 760 mm Hg, °C	307.8	290.0	278.3	340.0	360.0
Vapor pressure (20°C), mm Hg	1.17×10^{-5}	5.55×10^{-5}	8.12×10^{-4}	6.59×10^{-5}	7.67×10^{-7}
Temperature at which vapor pressure is 10^{-5} mm Hg, °C	18.7	7.5		3.7	
Liquid density g/cm^3	1.125	1.265	1.125	1.048	0.891
Latent heat of evaporation, cal/gm	109.9	196.3	114.1	63.8	64.4
Diffusion coefficient, 20°C, cm^2/sec vapor in air	.056	.086	.064	.046	.040
Refractive index	1.45	1.48	1.46	1.49	1.46
Solvents	H_2O	H_2O	H_2O	organic solvents	organic solvents

this size would spiral outward very slowly and essentially would remain in the vortex cores. Liquid droplet lifetimes of about 300 sec are required to mark vortices. Nontoxic hygroscopic liquids with the desirable evaporative characteristics have been identified.

Flight tests and studies of the dispersibility and fate of marker molecules in the atmosphere will be required to evaluate the suitability of this technique for marking trailing vortices.

For night or low visibility with cloud formation, rain, fog, or dense smog, radar or infrared devices would need to be considered.

References

[1] Vortex Wake Turbulence--Flight Tests Conducted During 1970' FAA Report No. FAA-FS-71-1, FAA Flight Standards Service, Washington, D.C. Feb. 1971, AD 724589.

[2] McGowan, W.A., "NASA Aircraft Trailing Vortex Research," *Symposium on Turbulence*, Federal Aviation Administration, Washington D.C., March 22-24, 1971, N72-29228.

[3] Spreiter, J.R. and Sacks, A.H. "The Rolling Up of the Trailing Vortex Sheet and Its Effect on the Downwash Behind Wings," *Journal of the Aeronautical Sciences*, Vol. 18, Jan. 1951, pp. 21-32.

[4] MacCready, P.B., Jr., "An Assessment of Dominant Mechanisms in Vortex-Wake Decay," *Aircraft Wake Turbulence and its Detection*, edited by J.H. Olsen, A. Golderg, and M. Rogers, Plenum Press, N.Y. 1971, pp. 289-304

[5] Garodz, L.J., "Federal Aviation Administration Full-Scale Aircraft Vortex Wake Turbulence Flight Test Investigations: Past, Present, Future," AIAA Paper 71-97, N.Y. 1971.

[6] McCormick, B.W., Tangler, J.L., and Sherrieb, H.E., "Structure of Trailing Vortices," *Journal of Aircraft*, Vol. 5, March 1968, pp. 260-267.

[7] Mason, W.H. and Marchman, J.F., "Far-Field Structure of Aircraft Wake Turbulence," *Journal of Aircraft*, Vol. 10, Feb. 1973, pp. 86-92.

[8] Corsiglia, R.R., Schwind, R.G., and Chigier, N.A., "Rapid Scanning, Three-Dimensional Hot-Wire Anemometer Surveys of Wing-Tip Vortices," *Journal of Aircraft*, Vol. 10, Dec. 1973, pp. 752-757.

[9] Ciffone, D.L. and Orloff, K.L., "Far-Field Wake-Vortex Characteristics of Wings," *Journal of Aircraft*, Vol. 12, May 1975, pp. 464-470.

[10] Donaldson, C. duP., *A Brief Review of the Aircraft Trailing Vortex Problem*, Aeronautical Research Associates of Princeton, N.J., Rept. 155, May 1971.

[11] Crow, S.C., "Stability Theory for a Pair of trailing Vortices," *AIAA Journal*, Vol. 8, Dec. 1970, pp. 2172–2179.

[12] Mager, A., "Dissipation and Breakdown of a Wing-Tip Vortex," *Journal of Fluid Mechanics*, Vol. 55, 1972, pp. 609-628.

[13] Chevalier, H., "Flight Test Studies of the Formation and Dissipation of Trailing Vortices," *Journal of Aircraft*, Vol. 10, Jan. 1973, pp. 14-18.

[14] Tombach, I., "Observations of Atmospheric Effects on Vortex Wake Behavior," *Journal of Aircraft*, Vol. 10, Nov. 1973, pp. 641-647.

[15] Patterson, J.C., Jr., personal communication, Langley Research Center, Hampton, Va., Aug. 1974.

[16] Mie, G., "Beitrage zur Optik trüber Medien," *Annalender Physik*, Vol. 25, 1908, pp. 377-445.

[17] Born, M. and Wolf, E., *Principles of Optics*, Pergamon Press, 4th Ed., 1970, p.633.

[18] Van De Hulst, H.C., *Light Scattering by Small Particles*, Wiley, N.Y. 1957, p. 5.

[19] Paranjpe, G.R., Naik, Y.G., and Vaidya, P.B., "Scattering of Light by Large Water Drops, Parts I and II," *Indian Academy of Sciences, Proceedings A*, Vol. 9, 1939, pp. 333-364.

[20] Sinclair, D. and La Mer, V.K., "Light Scattering as a Measure of Particle Size in Aerosols," *Chemical Reviews*, Vol. 44, 1949, pp. 245-267.

[21] Heller, W., "Theoretical and Experimental Investigation of the Light Scattering of Collodial Spheres," *ICES Electromagnetic Scattering*, Edited by M. Kerker, MacMillan, N.Y. 1963, pp. 101-120.

[22] Moon, P., *The Scientific Basics of Illuminating Engineering*, Dover, N.Y., 1961, p. 49.

[23] Gumprecht, R.O., and Sliepcevich, C.M., *Tables of Light-Scattering Functions for Spherical Particles*, Engineering Research Institute., Ann Arbor Mich., 1951.

[24] Holl, H., "Lichtstreuung an Dielektrischen Kugeln vom Brechungsexponenten $n=4/3$," *Optik*, Vol. 1, 1946, pp. 213-226.

[25] Green, H.L. and Lane, W.R., *Particulate Clouds: Dusts, Smokes and Mists*, 2nd Ed., Van Nostrand Co., Princeton, N.J., 1964, p. 444.

[26] Bate, E.R., Jr., *Aircraft Wake Modeling: Preliminary Design Aspects*, AeroVironment Inc., Pasadena, Calif., Report AV FR 445, Aug. 1974.

[27] Hoffmann, E.R. and Joubert, P.N., "Turbulent Line Vortices," *Journal of Fluid Mechanics*, Vol. 16, July 1963, pp. 395-411.

[28] Kent, J.C., "Quasi-Steady Diffusion-Controlled Droplet Evaporation and Condensation," *Applied Scientific Research*, Vol. 28, Nov. 1973, pp. 315-360.

[29] Marshall, W.R., Jr., "Heat and Mass Transfer in Spray Drying," *Transactions of the ASME*, Vol. 77, Nov. 1955, pp. 1377-1385.

[30] Moore, D.W., "Finite Amplitude Waves on Aircraft Trailing Vortices," *Aeronautical Quarterly*, Nov. 1972, pp. 307-314.

[31] Garodz, L.J., "Measurements of Boeing 747, Lockheed C5A and Other Aircraft Vortex Wake Characteristics By Tower Fly-By Technique," *Aircraft Wake Turbulence and Its Detection*, edited by J.H. Olsen, A. Goldburg, and M. Rogers, Plenum Press, N.Y. 1971, pp. 265-285.

[32] *Aviation Week and Space Technology*, Vol. 96, March 13, 1972, pp. 103.

[33] Condit, P.M. and Tracy, P.W., "Results of the Boeing Company Wake Turbulence Test Program," *Aircraft Wake Turbulence and Its Detection*, edited by J.H. Olsen, A. Goldburg, and M. Rogers, Plenum Press, N.Y., 1971, pp. 473-508.

[34] Perry, R.H. and Chilton, C.H., *Chemical Engineers' Handbook*, McGraw-Hill, N.Y., 5th Ed., 1973.

[35] *The Merck Index*, 7th ed., Merck Co., 1960.

[36] Barber, M. R., private communication, NASA Flight Research Center, Edwards, Cal.

[37] Barber, M.R., Kurkowski, R.L., Garodz, L.J., Robinson, G.H., Smith, H.J., Jacobsen, R.A., Stinnett, G.W., Jr., McMurtry, T.C., Tymczyszyn, J.J., Devereaux, R.L., and Bolster, A.J. ,"Flight Test Investigation of the Vortex Wake Characteristics Behind a Boeing 727 During Two-Segment and Normal ILS Approaches," (a joint NASA FAA Report) NASA TMX-62, 398, Jan. 1975, (N75-17340).